Screening theory based modeling of the quantum Hall based quasi-particle interferometers defined at quantum-dots

A. Salman[a,*], E. Koymen[a], M. B. Yucel[a], H. Atci[b], U. Erkarslan[b], A. Siddiki[c,d]

[a]*Akdeniz University, Faculty of Sciences, Physics Department, Antalya 07058, Turkey*
[b]*Mugla University, Faculty of Sciences, Physics Department, Kotekli 48170, Mugla, Turkey*
[c]*Istanbul University, Faculty of Sciences, Physics Department, Vezneciler-Istanbul 34134, Turkey*
[d]*Harvard University, Physics Department, Cambridge 02138 MA, USA*

Abstract

In this work, we investigate the spatial distributions and the widths of the incompressible strips, `i.e.` the edge-states. The incompressible strips that correspond to $\nu = 1, 2$ and $1/3$ filling factors are examined in the presence of a strong perpendicular magnetic field. We present a microscopic picture of the fractional quantum Hall effect based interferometers, within a phenomenological model. We adopt Laughlin quasi-particle properties in our calculation scheme. In the fractional regime, the partially occupied lowest Landau level is assumed to form an energy gap due to strong correlations. Essentially by including this energy gap to our energy spectrum, we obtain the properties of the incompressible strips at $\nu = 1/3$. The interference conditions are investigated as a function of the gate voltage and steepness of the confinement potential, together with the strength of the applied magnetic field.

Keywords: Quantum Hall effect, Edge states, Quasi-particles

PACS: 73.43.-f, 73.23.-b, 73.43.Cd

1. Introduction

The quantum behavior of particles has attracted many concern; one of these concern is the quantum Hall based interferometers which are realized in the two dimensional electron systems (2DESs). The discovery of the integer [1] and fractional [2] quantum Hall effects paved the path to investigate the importance of interactions, in particular, by intensive efforts related with the transport phenomena in the 2DES. At low temperatures and at certain magnetic field intervals, it is observed that the Hall conductance σ_{xy} assumes quantized values in units of e^2/h, whereas the longitudinal conductance σ_{xx} vanishes. The experimental realization of the integer quantum Hall effect (IQHE) shows that the constant Hall conductance occurs if the electron number density $n_{\rm el}$ is an integer (i) multiple of the magnetic flux density n_{Φ_0}. This ratio is named as the filling factor, $\nu = n_{\rm el}h/eB$ and it describes the Landau level filling at a given magnetic field. In the integer regime, i.e. if $\nu = i$, it means that the Fermi energy falls between the two adjacent

*Corresponding Author. Tel.: +902423102288; Fax: +902422278911
Email address: `aysevil@akdeniz.edu.tr` (A. Salman)

Landau levels and the electrostatic potential cannot be screened, the electron density remains constant. This state is called incompressible. If Fermi energy equals to a Landau level, the screening ability is good and this state is called compressible. In the fractional quantum Hall effect (FQHE) regime, the Landau level is partially occupied, hence, $\nu = f$. At certain fractional filling factors, it has been shown that this partially occupied highly degenerate Landau level splits into degenerate sub levels, and energy gaps are formed. These gaps lead also an incompressible state.

In 1982, Wilczek introduced a new kind of statistical particles named anyons [3, 4], which is described by fractional statistics in two dimensions. The quantum mechanics of anyons are formulated by including a statistical interaction potential to the Lagrangian or Hamiltonian of ordinary particles [5]. According to the quantum field theory of anyons, the electromagnetic potential is replaced by the Chern-Simons field. The Chern-Simons field is defined by the composite-particle (fermion or boson) field that represents anyons. In the case of a two dimensional electron gas subject to strong perpendicular magnetic field, these anyonic particles are called Laughlin quasi-particles (LQPs) which obey fractional statistics and have an effective fractional electric charge $e^* = e/(2i + 1)$. Laughlin describes the Landau level filling for FQH states as $f = 1/(2i + 1)$ where i is an integer [6] and LQPs are described by elementary charged excitations of FQH condensate [7].

The "quantum Hall" based interferometers, has revealed a novel technique to exploit the properties of the quasi-particles, which utilizes the so called edge states (ESs) in the extreme quantum limit. The ESs are considered as monochromatic (-energetic) beams that carry quasi-particles without scattering. Therefore, the overall interference pattern also strongly depends on the spatial distribution of these states. To understand the properties of Laughlin quasi-particles, a number of experiments has been performed by Camino et al. [7–9]. A key element of these experiments are the quantum point contacts (QPCs) and the electrostatic potential profile near these QPCs together with the quantum dot. Electrostatics play an important role on the formation and the spatial rearrangement of the electrostatic potential. Moreover, the interaction of the electrons or quasi-particles was proposed to be a possible origin of the dephasing and a better understanding requires a self-consistent (SC) calculation of the electrostatic potential [10]. Here we present an implementation of the SC-Thomas-Fermi-Poisson approach to investigate the effects induced by direct Coulomb interactions considering an homogeneous 2DES, where the interferometer is defined by a quantum dot.

2. The Model

The electrostatic treatment of the ESs is handled analytically by Chklovskii, Shklovskii and Glazman (CSG) [11]. In their pioneering work, they developed an electrostatic model considering the gate defined samples and studied the formation of edge states. Using the stability condition of the electrostatic potential, they obtained the positions and the widths of the incompressible states, which resemble the edge states. They argued that their results can be employed to the etched structures by using appropriate gate voltages that simulating etched edges [11]. Subsequently, Gelfand and Halperin (GH) studied the edge electrostatics and investigated the distribution of electron density considering an

etching defined sample [12]. Both of the theories are accepted to be viable also for FQHE [11, 12]. In a recent work, the positions and the widths of incompressible states are studied by Salman et al for both cases investigating a regular Hall bar, utilizing a self-consistent numerical approach [13]. There, it is shown that the predictions of the charge density profile within the analytical approximations deviate considerably from the self-consistent calculations.

In this work, we employ the commonly used self-consistent Thomas-Fermi-Poisson approach (SCTFPA) to obtain the electrostatic potential and the electron distribution in the structures. The total potential energy that electron experiences, within a mean-field approximation, is

$$V(x,y,z) = V_d(x,y,z) + V_g(x,y,z) + V_{\text{surf}}(x,y,z) + V_{\text{int}}(x,y,z), \tag{1}$$

here, $V_d(x,y,z)$ is generated by the ionized donors, $V_g(x,y,z)$ is due to metallic gates deposited on the surfaces, $V_{\text{surf}}(x,y,z)$ represents the surface potential and the last term stands for the electron-electron interactions, which is determined by the electron density distribution $n_{\text{el}}(x,y,z)$. The surface and gate potentials are fixed by the sample properties, e.g. the surface potential is determined by the mid-gap energy of the heterostructure. The potential generated by the charges are calculated via solving the Poisson's equation for given boundary conditions numerically.

In our self-consistent calculation scheme, we fix the homogeneous immobile charge distribution, i.e. the donors; then the electron density profile is calculated by the electrostatic potential emanating from the donors, surface and gates. Next, the electrostatic potential is determined by the electron density profile in a self-consistent loop, at zero magnetic field and temperature. To start the self-consistent calculation we focus on the lithographically defined sample, resembling the experimental structures [7–9]. By considering the crystal growth parameters together with the surface image of the quantum dot pattern, we calculate the charge distribution at the 2DES. The details of the self-consistent process are given in Ref. [14–16].

The next step is to determine the spatial positions of the edge states, which is a straightforward procedure when the electron density distribution is known. Our self-consistent scheme provides this information, and integer or fractional filling factors (the edge states) can be found simply by $\nu(x,y) = 2\pi\ell^2 n_{\text{el}}(x,y,z = \text{2DES})$; here $\ell = \sqrt{\hbar/eB}$ is the magnetic length. In a further step, one can calculate also the widths of the incompressible edge states, by following the pioneering work of Chklovskii et al [11] given as

$$a_{i,f} = \sqrt{\frac{2\epsilon\Delta E_{i,f}}{\pi^2 e^2 dn/dx|_{x=x_{i,f}}}} \tag{2}$$

where $\Delta E_{i,f}$ is the energy gap, assuming the Zeeman split Landau gap for the integer case and the many-body effects induced gap for the fractional case.

Aharonov-Bohm interferometers (ABI) are basically used to measure the vector potential induced phase difference between two paths of the (quasi-)particles. The single electron states at the Landau level are quantized by the Aharonov-Bohm condition and determines the phase, whereas for the LQPs the phase is determined by the properties of the composite particle [8]. In the existence of a perpendicular magnetic field, the closed paths define an area $S = \pi r^2$ with radius r that encircles the magnetic flux Φ and is given by $\Phi = BS\,m = m\Phi_0$. The encircled area of

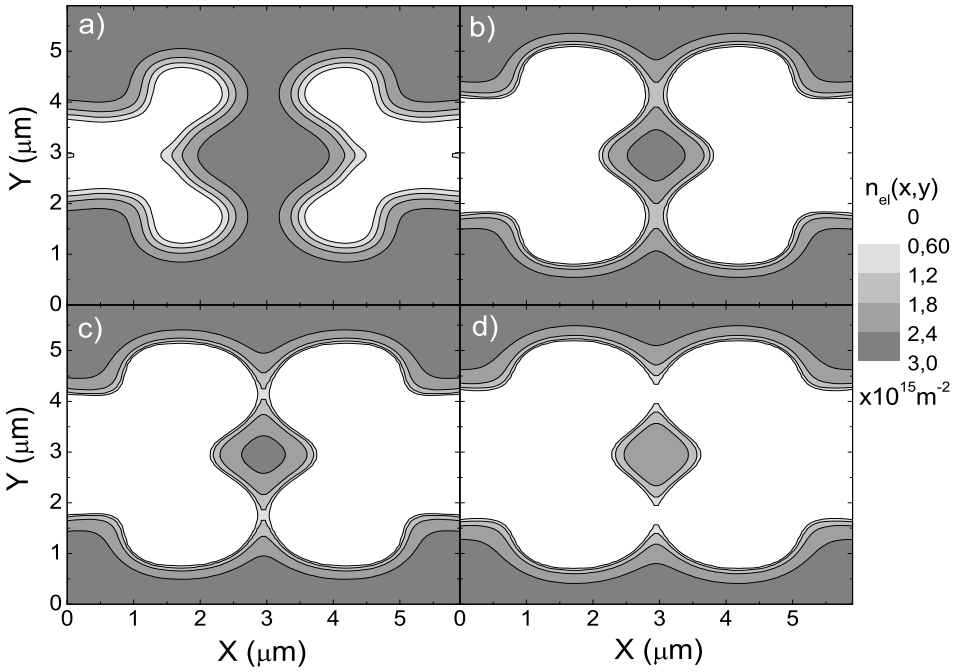

Figure 1: (Color online) Spatial distribution of electrons at zero magnetic field and zero temperature. (a) gated sample where potential is fixed to $V_g = -2.0V$. (b) and (c) etched structures, whose etching depths are 160 nm and 240 nm from the surface of the sample, respectively. (d) etched and also gated (trench gated) sample: etching depth is 240 nm, gate voltage is $-2.0V$.

the orbital is given by S_m and m represents the quantum numbers of the orbital, where $\Phi_0 = h/e$ is the magnetic flux quantum [8]. The theoretical predictions by Aharonov and Bohm [17] states that the interference between the two paths depends on the phase difference, and the phase difference is given by the integer multiples of the magnetic flux quanta Φ encircled. Therefore, the area of an orbit is $S_m = 2\pi m\ell^2$ where ℓ is the radius of the orbit [18]. The region between the two adjacent orbits is $S_{m+1} - S_m = h/eB$, and this is related with the occupation of these orbits which is given by the filling factor as described above, *i.e.* $\nu = 2\pi\ell^2 n_{\rm el}$. Therefore, it is essential to find the exact locations of integer or fractional edge states to pin down the area enclosed by the interference paths. In the following section, the spatial distributions of the edge states will be provided by considering real experimental parameters.

3. Results and Discussion

The physical area of the structure that we considered is 5.9 μm× 5.9 μm, and the 2DES is 280 nm below the surface in z direction, similar to the experimental case [7–9]. The 2DES is generated at the interface of the GaAs-AlGaAs heterostructure. Hence, we set the Lande-g* factor to be -0.44, as default. We obtain the electron densities self-consistently as mentioned above. Typical electron density distributions are shown in Fig 1, (a) considering gate,

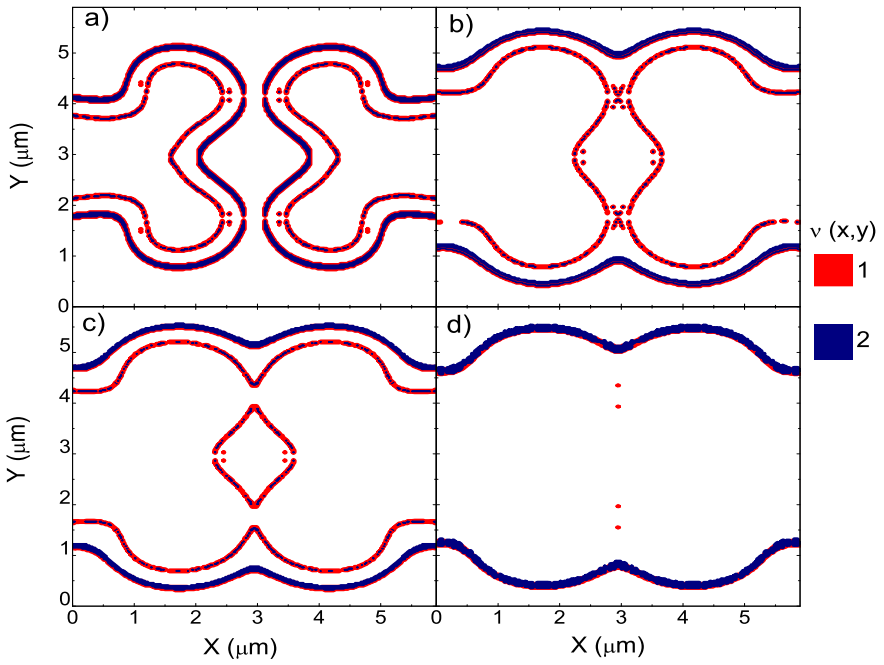

Figure 2: (a) and (b) show the spatial distribution of ISs for gated samples at 2.6 T magnetic field. $V_g = -2.0V$ in (a) and $V_g = -5.0V$ in (b). (c) and (d) show the spatial distribution of ISs for 160nm etched and also -2.0V potential is applied (trench gated) sample. The magnetic field is 2.6 T in (c) and 5.1 T in (d).

(b) shallow etched, (c) deep etched and (d) trench gate (i.e. first etched then gated) defined samples. The gray scale depicts the electron occupied regions, whereas white areas denote the electron depleted regions. Here, the physical dimensions of the surface pattern are taken to be the same.

Since the electron free (white) regions are dominant in (b-d) one can conclude from Fig. 1 that, etching is more effective in depleting electrons when it is compared to solely gate defined quantum dots. Note that, to manipulate the electron density distribution, hence the area, one needs to impose metallic gates biased by negative voltages. Therefore, we also show the trench gated samples, resembling the experiments. This method is the most powerful technique to investigate both the edge effects and interference phenomena. In our calculations, we follow the arguments of Gerhardts [19], Fogler [20] and Chang [21] in describing the non-equilibrium current. We assume that the current is carried by incompressible regions, since scattering is completely suppressed due to the lack of available states at the Fermi energy. However, our calculations are also viable if one utilizes the Landauer-Büttiker picture for transport and considers solely the capacitive effects proposed by Halperin and his co-workers [22, 23].

Fig. 2 shows the ESs considering the filling factors $\nu = 1$ and 2. To find the spatial distribution of the incompressible strips, we imposed magnetic field values 2.6 T and 5.1 T, that are consistent with the experiments [8]. As it is seen from Fig. 2, there are two edge channels (inner (light) and outer (dark)). The outer edge channel corresponds to

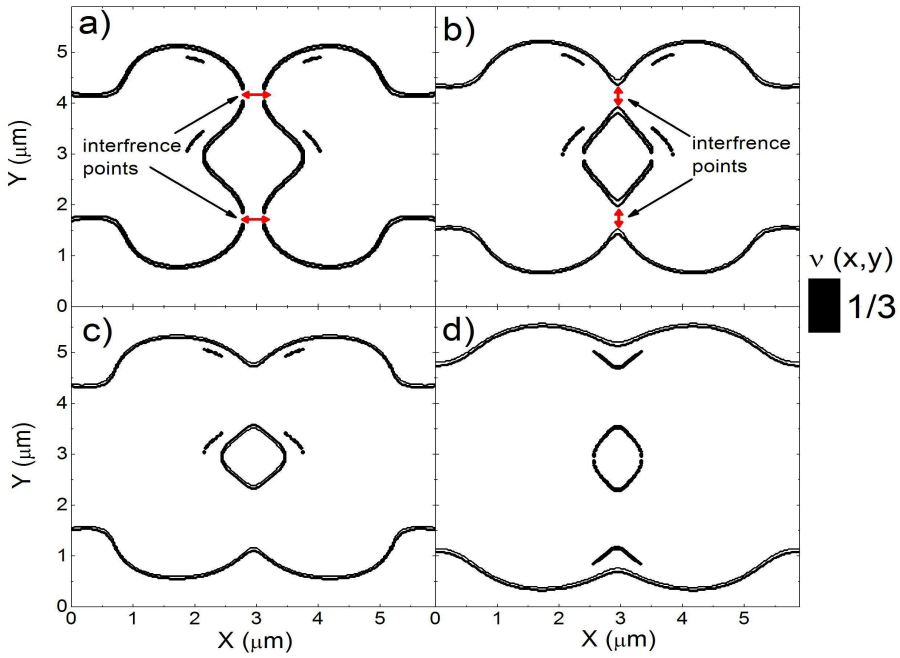

Figure 3: Spatial distribution of the incompressible strips for $\nu = 1/3$ state at different gate voltages. In (a) $V_g = -3.0V$, (b) $V_g = -4.0V$, (c) 160 nm etched sample is considered at 14.4 T (d) 160 nm etched and also $V_g = -4.0V$ gated sample is considered at 14.4 T.

$\nu = 2$ and inner edge channel corresponds to $\nu = 1$. At relatively low gate voltages, Fig. 2a, the both edge channels are transmitted through the constrictions, whereas at higher negative gate voltages (Fig. 2b) the outer edge state is back-reflected; meanwhile, the inner edge states come closer to each other and start to overlap. Thus, the interference is more possible for lower gate voltages, at least for the inner channel. In Fig. 2b, we observe that the inner channels overlap, whereas the outer channels are (back-)reflected, hence, at this configuration tunneling becomes impossible for $\nu = 2$ state. Fig. 2c and Fig. 2d depict the results for trench gated samples (160 nm etched and -2.0 V is applied to the gates). The outer edge channels are decoupled, hence interference is suppressed. Also in Fig. 2d, the inner edge channels disappear due to the steepness of the electron density that is considered for trench gated samples. The incompressible strip is very narrow compered to the magnetic length under these conditions, and the inner edge channel is therefore suppressed. For high magnetic fields none of the channels are transmitted, therefore, interference is completely washed out.

We also investigate the $\nu = 1/3$ edge state in the presence of strong magnetic fields. We showed that it is more possible to observe the interference at $\nu = 1/3$, particularly at gated samples by imposing low gate voltages, Fig. 3a. When the gate voltages are increased, electrons are repelled more from the edges, therefore, the edge states on the left and right start to overlap. Etching also depletes the electrons more sharply than gating as a result of steeper potential

gradient, hence, the quasi-particle edge states overlap. If the sample is made by the trench gated as shown in Fig. 3d, it is observed that the edge states are dispelled the most effectively.

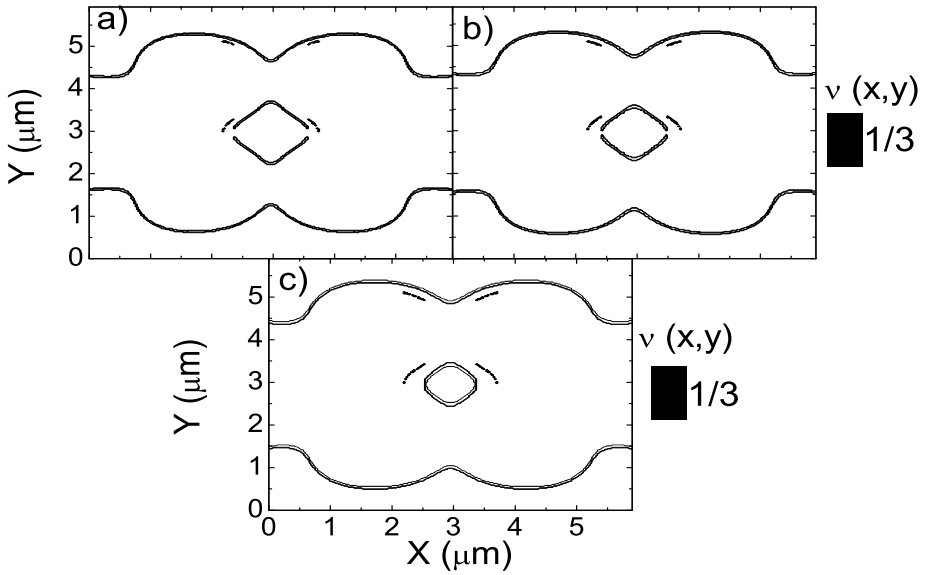

Figure 4: Spatial distribution of the incompressible strips for $\nu = 1/3$ state in 240 nm etched sample with different magnetic field values: (a) B=12.0 T, (b) B=13.2 T (c) B=14.4 T.

In a further investigation, we studied the effect of magnetic field on the path of the edge states, hence the enclosed area. The distribution of $\nu = 1/3$ edge state is shown in Fig. 4. The calculated areas of the enclosing loops in Fig. 4 are 1.04 μm^2 for (a), 0.78 μm^2 for (b) and 0.45 μm^2 for (c). It is interesting to observe that, by changing magnetic field monotonously, the actual area enclosed by the $\nu = 1/3$ edge state changes approximately by a factor of 2. Therefore, assuming an area independent charging model seems not to be plausible. However, one should also keep in mind that in actual experiments, the interference signal is not observed in a large B interval. This is due to the fact that not only the area is changed, but also the tunneling mechanisms are altered. To be explicit, while the magnetic field varied, one also suppresses the scattering between the edge states by pulling them apart. Hence, no partitioning can take place and interference signal disappears. Therefore, one cannot measure the phase difference between two paths. This observation, of course, does not hinder the fact that the area enclosed is strongly affected by the change of magnetic field.

4. Conclusions

In this work, we numerically investigated the electrostatics of a field effect induced quantum dot, and hence, the spatial distribution of the edge states by considering the Aharonov-Bohm interference experiments performed in the

integer ($\nu = 1, 2$) and fractional ($\nu = 1/3$) quantized Hall regimes [7, 8]. We observed that, defining the interference device (i.e. the quantum dot) which is created by trench gating provides a steeper edge potential profile, and therefore, this device is more effective for interferometric measurements. In contrast, the gate defined devices enables higher visibility at fractional states, due to the fact that these states become more stable since the density gradients are smoother. Another observation is related with the change of the area while sweeping the magnetic field. At the integer regime, edge states are less affected by the change in B, hence capacitive models that essentially neglect the areal dependency may become more reliable. Our final remark for the fractional case is, the area changes approximately a factor of 2 while changing the magnetic field about 2.5 Tesla. Hence, an areal independent model is more questionable.

The observations yield the following conclusion: To investigate the importance of the areal dependency, therefore the importance of Hartree type interactions, it is necessary to perform experiments with the same sample geometry for the both gate and trench gated samples. We expect to see that the gate defined samples will show an enhanced areal dependency, due to the fact that their edge potential profile are smoother.

Acknowledgments

This work is supported by the scientific and technological research council of Turkey under grant (TBAG:109T083) and Istanbul University IU-BAP:6970.

References

[1] K. v. Klitzing, G. Dorda, M. Pepper, New Method for High-Accuracy Determination of the Fine-Structure Constant Based on Quantized Hall Resistance, Phys. Rev. Lett. 45 (1980) 494-497.

[2] D.C. Tsui, H.L. Stormer, A.C. Gossard, Two-Dimensional Magnetotransport in the Extreme Quantum Limit, Phys. Rev. Lett. 48 (1982) 1559-1562.

[3] F. Wilczek, Magnetic Flux, Angular Momentum, and Statistics, Phys. Rev. Lett. 48 (1982) 1144-1146.

[4] F. Wilczek, Quantum Mechanics of Fractional-Spin Particles, Phys. Rev. Lett. 49 (1982) 957-959.

[5] Z. F. Ezawa, Quantum Hall Effects: Field Theoretical Approach and Related Topics, World Scientific Publishing Co., Singapore, 2008.

[6] R. B. Laughlin, Anomalous Quantum Hall Effect: An Incompressible Quantum Fluid with Fractionally Charged Excitations, Phys. Rev. Lett. 50 (1983) 1395-1398.

[7] F. E. Camino, W. Zhou, V. J. Goldman, e/3 Laughlin Quasiparticle Primary-Filling v = 1/ 3 Interferometer, Phys. Rev. Lett. 98 (2007) 076805/1-4.

[8] F. E. Camino, W. Zhou, V. J. Goldman, Aharonov-Bohm Electron Interferometer in the Hiqh Regime, Phys. Rev. B 72 (2005) 155313/1-6.

[9] F. E. Camino, W. Zhou, V. J. Goldman, Transport in the Laughlin Quasiparticle Interferometer: Evidence for Topological Protection in an Anyonic Qubit, Phys. Rev. B. 74 (2006) 115301/1-8.

[10] A. Siddiki, F. Marquardt, Self-consistent Calculation of the Electron Distribution Near a Quantum-point Contact in the Integer Quantum Hall Effect, Phys. Rev. B, 75, (2007) 045325/1-11.

[11] D. B. Chklovskii, B. I. Shklovskii, L. I. Glazman, Electrostatics of Edge Channels, Phys. Rev. B 46 (1992) 4026-4034.

[12] B. Y. Gelfand, B. I. Halperin, Edge Electrotatics of a Mesa-etched Sample and Edge-state-to-bulk Scattering Rate in the Fractional Quantum Hall Regime, Phys. Rev. B 49 (1994) 1862-1866.

[13] A. Salman, A. I. Mese, M. B. Yucel, A. Siddiki, An analytical model of fractional overshooting, arXiv:1012.1294 (2010).

[14] A. Siddiki, R. R. Gerhardts, Incompressible Strips in Dissipative Hall Bars as Origin of Quantized Hall Plateaus, Phys. Rev. B 70 (2004) 195335/1-12.

[15] A. Siddiki, R. R. Gerhardts, Thomas-Fermi-Poisson Theory of Screening for Laterally Confined and Unconfined Two-Dimensional Electron Systems in Strong Magnetic Fields, Phys. Rev. B 68 (2003) 125315/1-12.

[16] S. Arslan, E. Cicek, D. Eksi, S. Aktas, A. Weichselbaum, A. Siddiki Modeling of Quantum Point Contacts in High Magnetic Fields and with Current Bias Outside the Linear Response Regime, Phys. Rev. B 78 (2008) 125423/1-15.

[17] Y. Aharonov, D. Bohm, Significance of Electromagnetic Potentials in the Quantum Theory, Phys. Rev. Lett 115 (1959) 485-491.

[18] E. Cicek, A. I. Mese, M. Ulas, A. Siddiki, Spatial Distribution of the Incompressible Strips at AB Interferometer, Physica E 42 (2010) 1095-1098.

[19] K. Güven, R. R. Gerhardts, Self-consistent Local Equilibrium Model for Density Profile and Distribution of Dissipative Currents in a Hall Bar Under Strong Magnetic Fields, Phys. Rev. B 67 (2003) 115327/1-8.

[20] M. M. Fogler, B. I. Shklovskii, Resistance of a Long Wire in the Quantum Hall Regime, Phys. Rev. B 50 (1994) 1656-1662.

[21] A. M. Chang, A Unified Transport Theory for the Integral and Fractional Quantum Hall Effects: phase boundaries, edge currents, and transmission/reflection probabilities, Solid State Commun. 74 (1990) 871-876.

[22] I. Neder, M. S. Rudber, H. Bluhm, S. Foletti, B. I. Halperin, A. Yacoby Semi-classical Model for the Dephasing of at Two-electron Spin Qubit Coupled to a Coherently Evolving Nucleer Spin Bath, Phys. Rev. B 84, (2011) 035441/1-13.

[23] M. Buttiker, Four-Terminal Phase-Coherent Conductance, Phys. Rev. Lett. 57, (1986) 1761-1764.

FIGURE CAPTIONS

Figure 1: (Color online) Spatial distribution of electrons at zero magnetic field and zero temperature. (a) gated sample where potential is fixed to $V_g = -2.0V$. (b) and (c) etched structures, whose etching depths are 160 nm and 240 nm from the surface of the sample, respectively. (d) etched and also gated (trench gated) sample: etching depth is 240 nm, gate voltage is $-2.0V$.

Figure 2: a) and (b) show the spatial distribution of ISs for gated samples at 2.6 T magnetic field. $V_g = -2.0V$ in (a) and $V_g = -5.0V$ in (b). (c) and (d) show the spatial distribution of ISs for 160nm etched and also -2.0V potential is applied (trench gated) sample. The magnetic field is 2.6 T in (c) and 5.1 T in (d).

Figure 3: Spatial distribution of the incompressible strips for $\nu = 1/3$ state at different gate voltages. In (a) $V_g = -3.0V$, (b) $V_g = -4.0V$, (c) 160 nm etched sample is considered at 14.4 T (d) 160 nm etched and also $V_g = -4.0V$ gated sample is considered at 14.4 T.

Figure 4: Spatial distribution of the incompressible strips for $\nu = 1/3$ state in 240 nm etched sample with different magnetic field values: (a) B=12.0 T, (b) B=13.2 T (c) B=14.4 T.